

Supplementary material

Balancing uncertainty and complexity to incorporate fire spread in an eco-hydrological model

Maureen C. Kennedy^{A,B,E}, Donald McKenzie^C, Christina Tague^D and Aubrey L. Dugger^D

^AUniversity of Washington, School of Environmental and Forest Sciences, Box 352100
Seattle, WA 98195-2100, USA.

^BPresent address: University of Washington, School of Interdisciplinary Arts and Sciences,
1900 Commerce Street, Box 358436, Tacoma, WA 98402, USA.

^CPacific Wildland Fire Sciences Laboratory, Pacific Northwest Research Station, US Forest Service,
400 N 34th Street, Suite 201, Seattle, WA, USA.

^DUniversity of California, Santa Barbara, Bren School of Environmental Science and Management,
2400 University of California, Santa Barbara, CA 93117, USA.

^ECorresponding author. Email: mkenn@uw.edu

This supplementary document includes methods related to the calibration of the Regional Hydroecological Simulation System (RHESSys) for the two study sites, and for the estimation of empirical wind distributions. It also includes supplementary results and figures.

Supplementary methods

RHESSys calibration for Santa Fe and HJ Andrews

RHESSys has ecophysiological parameters such as photosynthesis that are typically assigned based on existing species-specific parameter libraries. Physical parameters in RHESSys are also typically specified based on input data layers (e.g. DEM). As with most watershed-scale hydrologic models, however, subsurface drainage parameters usually need to be calibrated by comparison with observed data (Tague *et al.* 2013; Garcia and Tague 2015). For each watershed, subsurface drainage parameters are optimised by comparing observed and modelled streamflow. These models are run using observed historical weather and climate data.

The implementation and calibration of RHESSys for SF has not been previously published, so we describe it here. For SF, RHESSys simulations were developed using vegetation and soil type maps from

the US Forest Service. Long-term historical climate inputs (1941–2007) included daily minimum and maximum air temperature and precipitation taken from two long-term climate stations in the City of Santa Fe (National Weather Service Cooperative Network, Santa Fe 1 and 2), scaled to the watershed using derived relationships between the Coop climate stations and two short-term SNOTEL stations within the watershed (Elk Cabin and Santa Fe). Calibration of subsurface drainage parameters followed the approach outlined in Tague and Peng (2013), using the period from 1999 to 2008 and calibrating to daily streamflow at USGS Gage 08315480 (Santa Fe River above McClure Reservoir). RHESSys performance for streamflow prediction over this 10-year period achieved a daily Nash–Sutcliffe efficiency of 0.7 (where a value of 1 corresponds to a perfect fit between observed and modelled streamflow) and mean bias of <5%. RHESSys-predicted vegetation dynamics were consistent with remotely sensed vegetation greenness indices and local tree-ring measurements.

The implementation and calibration of RHESSys for HJA used in this study is described in Garcia *et al.* (2013). Streamflow performance metrics show a long-term bias of less than 10%, and Nash–Sutcliffe efficiency for daily log-transformed streamflow of 0.85.

Estimation of empirical wind distributions

We use empirical wind distributions to estimate probability functions for wind speed and wind direction based on local weather station data. For wind speed, we fit the mean and standard deviation of log-normal distributions using the `fitdistr` function in the *R* statistical package. For wind direction, we fit a mixed von Mises circular distribution to each site, with a separate fit for the observed wind direction surrounding the two modes of wind direction observed at each site.

$$f(x | \mu, \kappa, p) = \hat{p} \times \frac{e^{\kappa_1 \cos(x - \mu_1)}}{2\pi I_0(\kappa_1)} + (1 - \hat{p}) \times \frac{e^{\kappa_2 \cos(x - \mu_2)}}{2\pi I_0(\kappa_2)} \quad (\text{S1})$$

where \hat{p} is the proportion of wind observations $< \pi$, I_0 is the modified Bessel function of order 0, x is the wind direction, μ_i ($i = 1, 2$) is the mean for each mode, and κ_i ($i = 1, 2$) is a measure of concentration about the mean in each mode (higher κ_i implies a more narrow distribution; Masseran *et al.* 2013). Estimated values for each watershed are given in Table S1.

Table S1. Estimated wind parameters for each watershed

μ_1 gives the mean and κ_1 a measure of concentration about the mean of the wind direction for the first mode of wind direction, and μ_2 gives the mean and κ_2 a measure of concentration about the mean for the second mode of wind direction (radians)

Watershed wind parameters	Mean log wind speed	s.d. log wind speed	μ_1	κ_1	μ_2	κ_2	\hat{p}
SF	1.64	0.55	1.9	6.43	−1.37	5.1	0.57
HJA	1.3	0.81	1.03	2.57	−1.74	2.37	0.4

For WMFire, we adapted the `rmixedvm` function (CircStats, see <https://CRAN.R-project.org/package=CircStats>) to draw a single prevalent wind direction from the bimodal distribution for each fire attempt each month, and then we draw from the log-normal distribution to obtain a single prevailing wind speed for each fire attempt.

LANDFIRE data

LANDFIRE is ‘a shared program between the wildland fire management programs of the US Department of Agriculture Forest Service and US Department of the Interior, providing landscape-scale geo-spatial products to support cross-boundary planning, management, and operations.’ (<https://www.LANDFIRE.gov/about.php>, accessed 2 March 2017). Its products include presumed historical fire regimes that are mapped using the Vegetation Dynamics Development Tool (VDDT).

We downloaded the fire regime group data layer (LANDFIRE 2014) to compare their presumed fire regimes with patterns predicted by WMFire, for each watershed (Table S2, Figs S1–S2). In SF, we see a spatial gradient, with increasing fire return interval from the lower to upper watershed, with low- to mixed-severity fire predicted throughout the watershed. In HJA, the entire watershed is in the fire regime groups characterised by fire return intervals >35 years.

Table S2. Fire Regime Groups (FRG) layer characterises the presumed historical fire regimes within landscapes based on interactions between vegetation dynamics, fire spread, fire effects, and spatial context (<https://www.LANDFIRE.gov/fireregime.php>)

Characteristics of each fire regime group and the proportion of pixels reported by LANDFIRE in each group for each study watershed are given below

Fire regime group	Characteristics	Proportion pixels SF	Proportion pixels HJA
1	≤35-year fire return interval, low and mixed severity	0.41	0.00
2	≤35-year fire return interval, replacement severity	0.00	0.00
3	35–200-year fire return interval, low and mixed severity	0.41	0.52
4	35–200-year fire return interval, replacement severity	0.16	0.00
5	>200-year fire return interval, any severity	0.00	0.48
Other	Includes water, snow and ice, barren, sparsely vegetated, or indeterminate	0.01	0.00

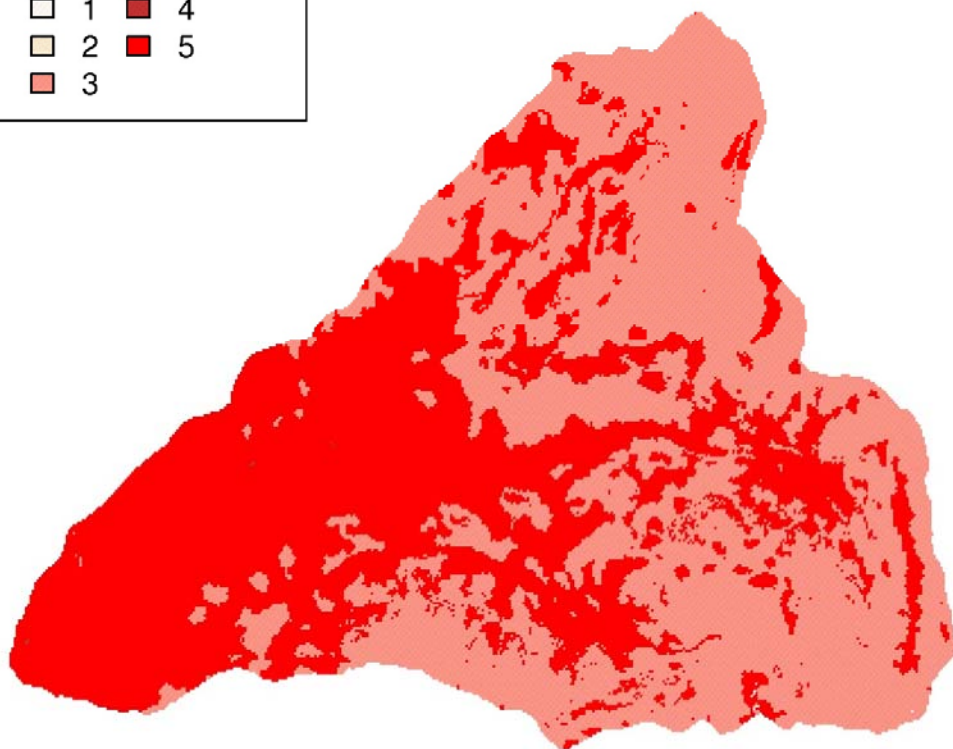


Fig. S1. LANDFIRE-inferred fire regime group for HJA (see Table S2 for description of each group). Note that throughout the watershed, the mean fire return interval is inferred to be >35 years, with spatial heterogeneity only in whether that return interval is <200 or >200 years.

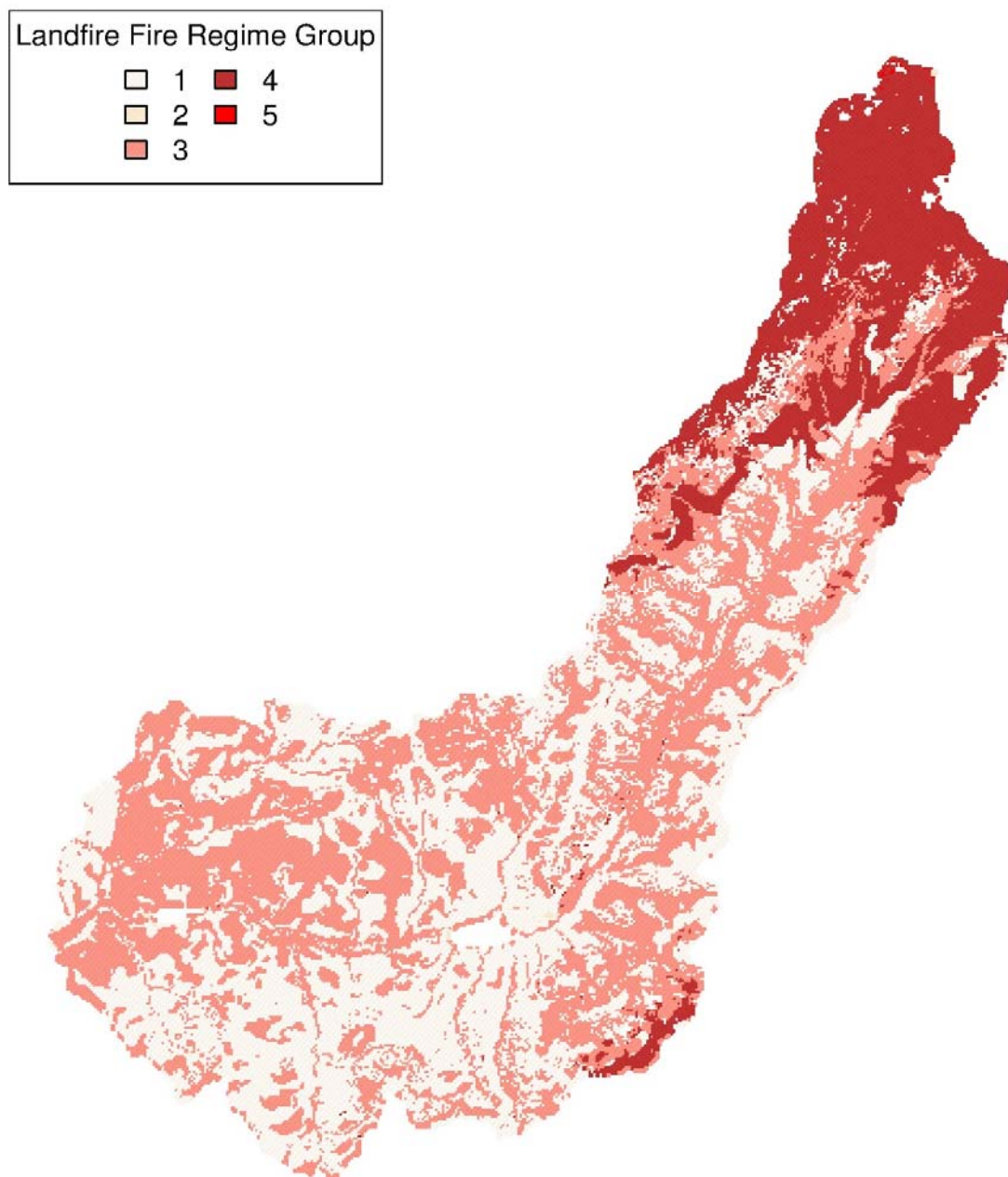


Fig. S2. LANDFIRE-inferred fire regime group for SF (see Table S2 for description of each group). Note the spatial gradient in fire regime group from the lower to upper watershed. At the lower watershed, return intervals are mixed between ≤ 35 years and between 35 and 200 years. All portions of the lower watershed are inferred to burn at low to mixed severity. In contrast, the upper watershed is inferred to burn at a 35–200-year interval with stand-replacement severity.

RHESys-predicted fuel load and relative deficit

RHESys predicts HJA to have higher fuel loads than SF (Fig. 1 in main manuscript). HJA shows more distinct seasonal patterns of deficit than SF (Figs S3–S4). The highest deficit in HJA is predicted in August, and the highest deficits in SF are predicted in June and July.

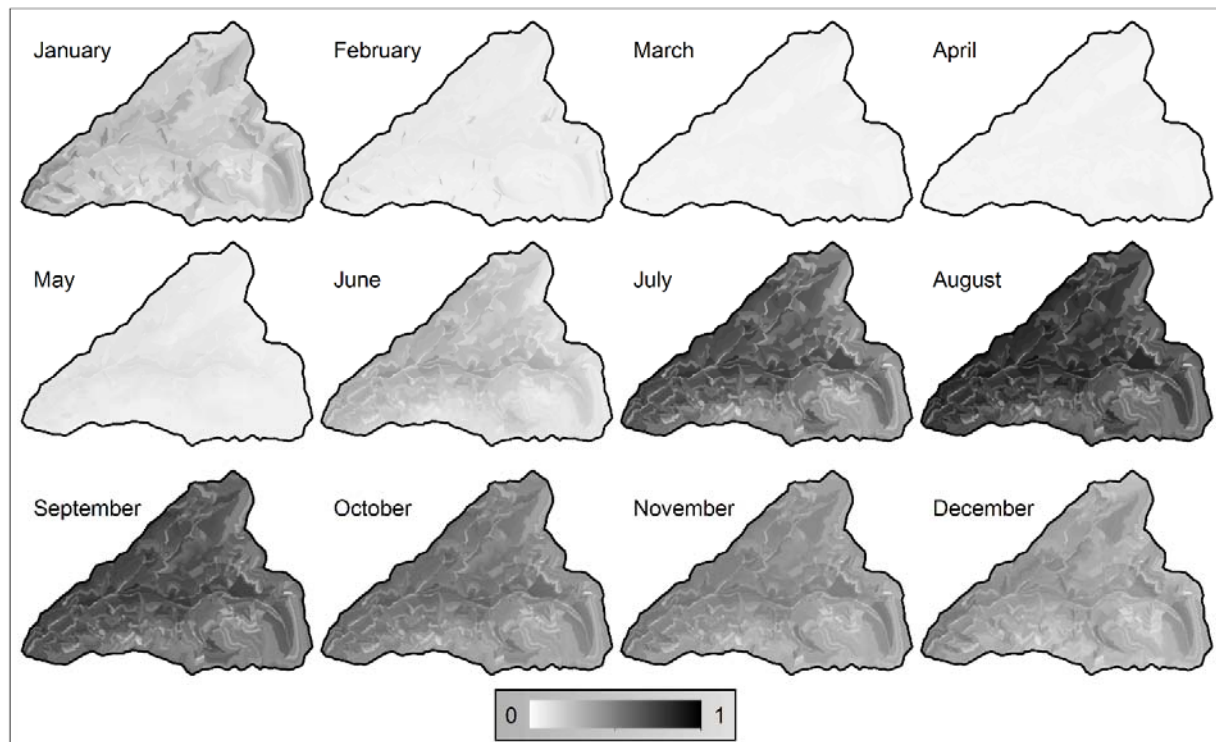


Fig. S3. Relative moisture deficit ($1 - ET/PET$) by month for HJA.

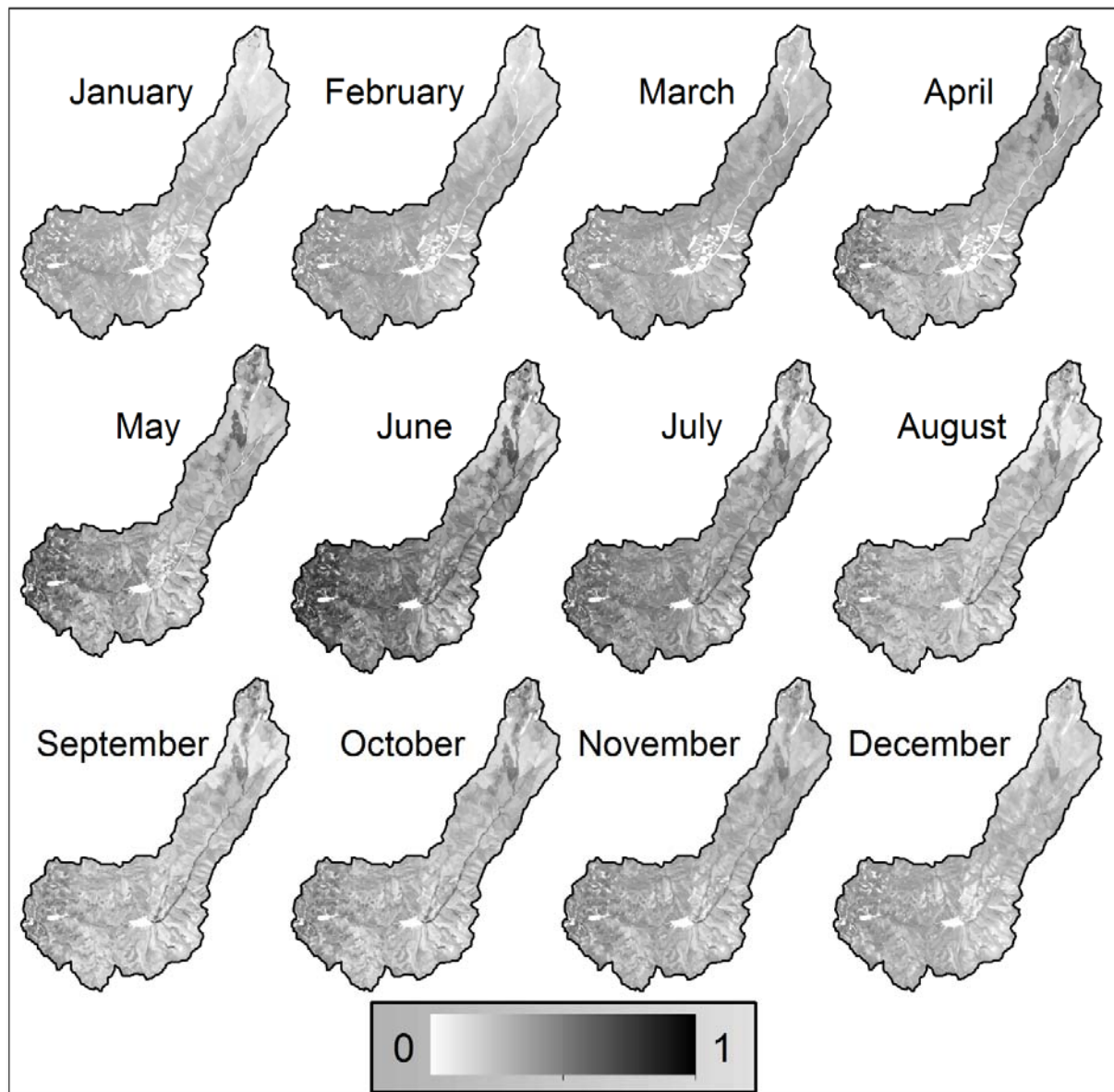


Fig. S4. Relative moisture deficit ($1 - ET/PET$) by month for SF.

Sensitivity of fire regime to ignition source rate

The season with the highest proportion of successful fire ignitions in each watershed is not sensitive to the mean ignition source rate, only the value that proportion takes is sensitive. The ignition source rate is the number of ignition sources tested for fire start per month. Figs S5–S10 show this point.

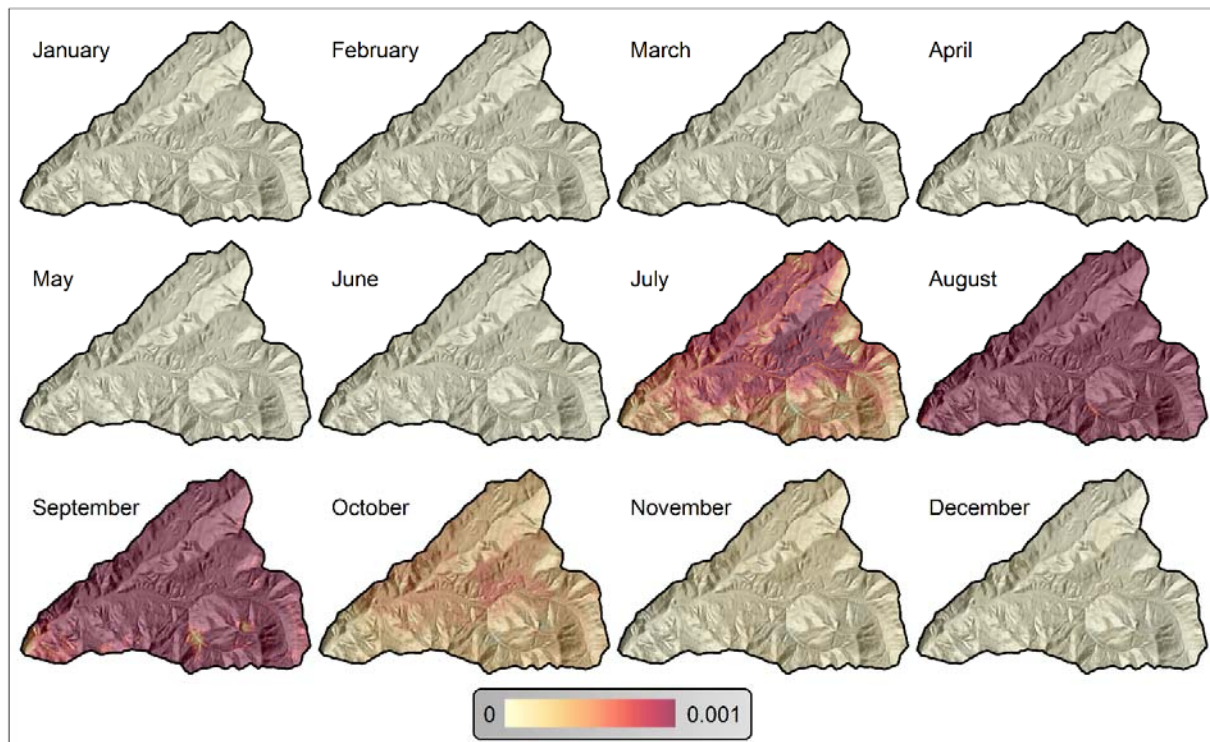


Fig. S5. Seasonality of HJA fire occurrence with an ignition source rate of 0.01. Values are the proportion of times each pixel experiences fire. Note the scale – these are the smallest proportions observed for any simulation.

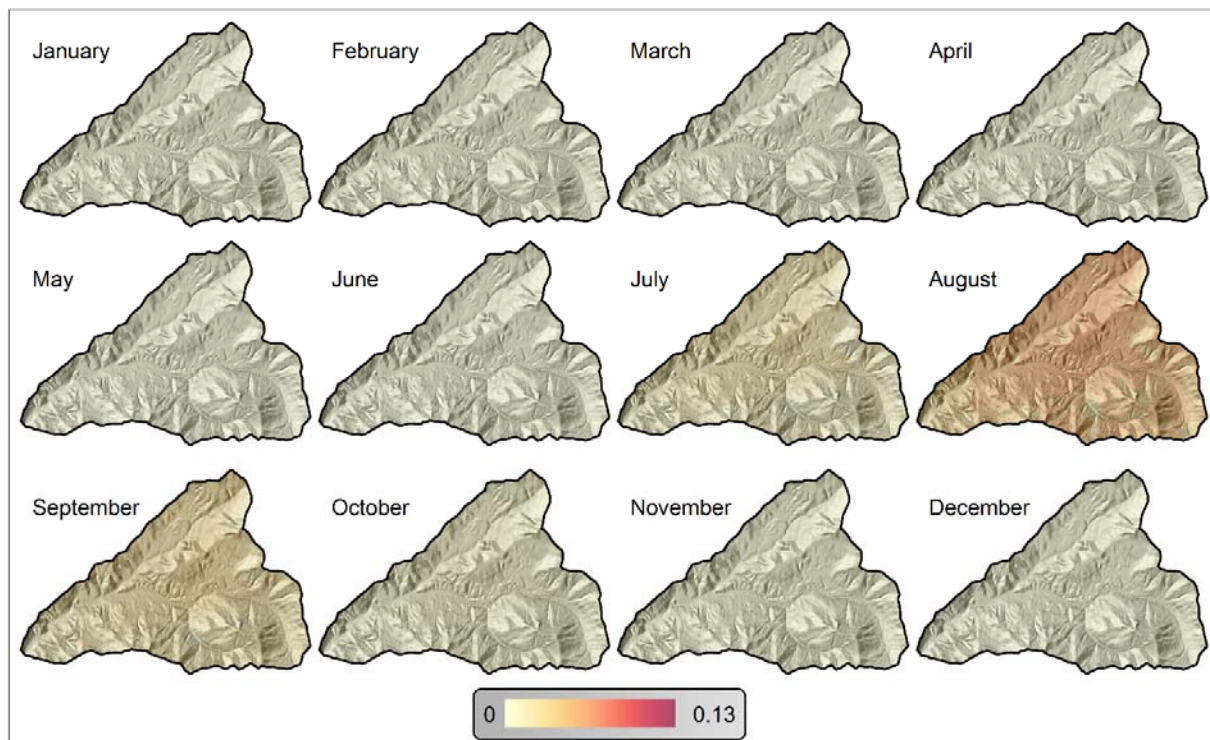


Fig. S6. Seasonality of HJA fire occurrence with an ignition source rate of 0.25. Values are the proportion of times each pixel experiences fire. Note the scale.

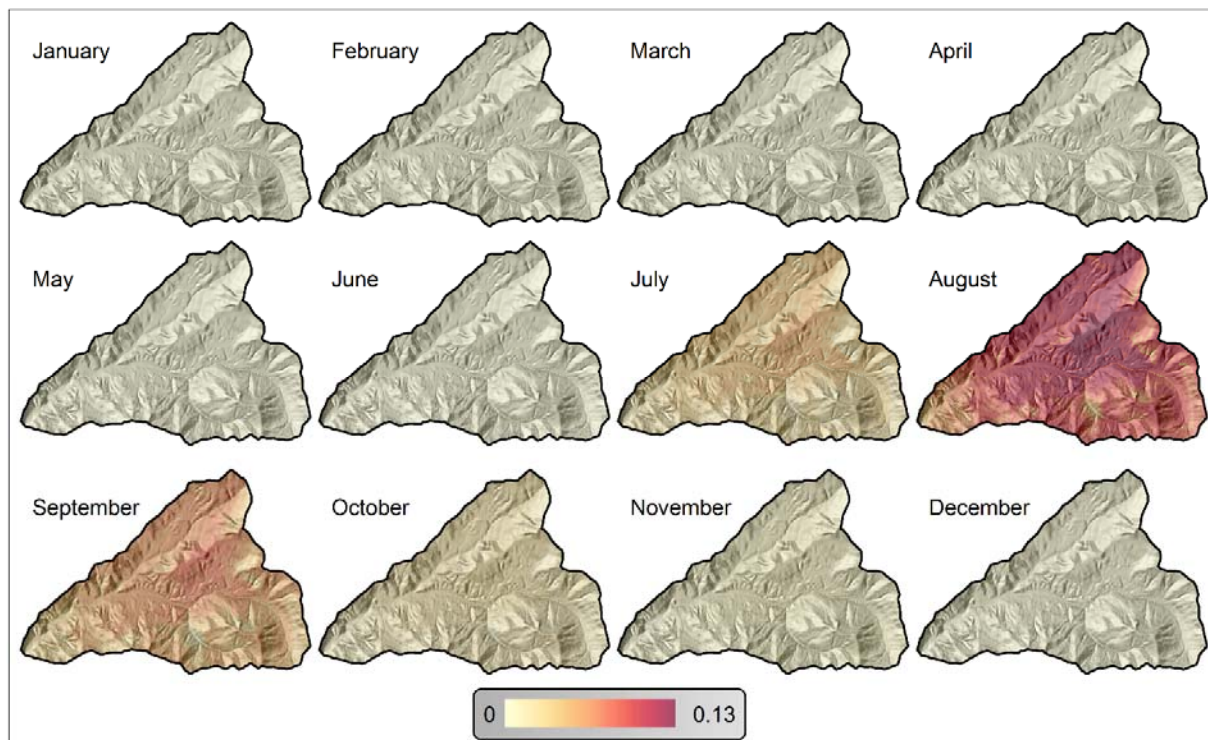


Fig. S7. Seasonality of HJA fire occurrence with an ignition source rate of 0.5. Values are the proportion of times each pixel experiences fire. Note the scale.

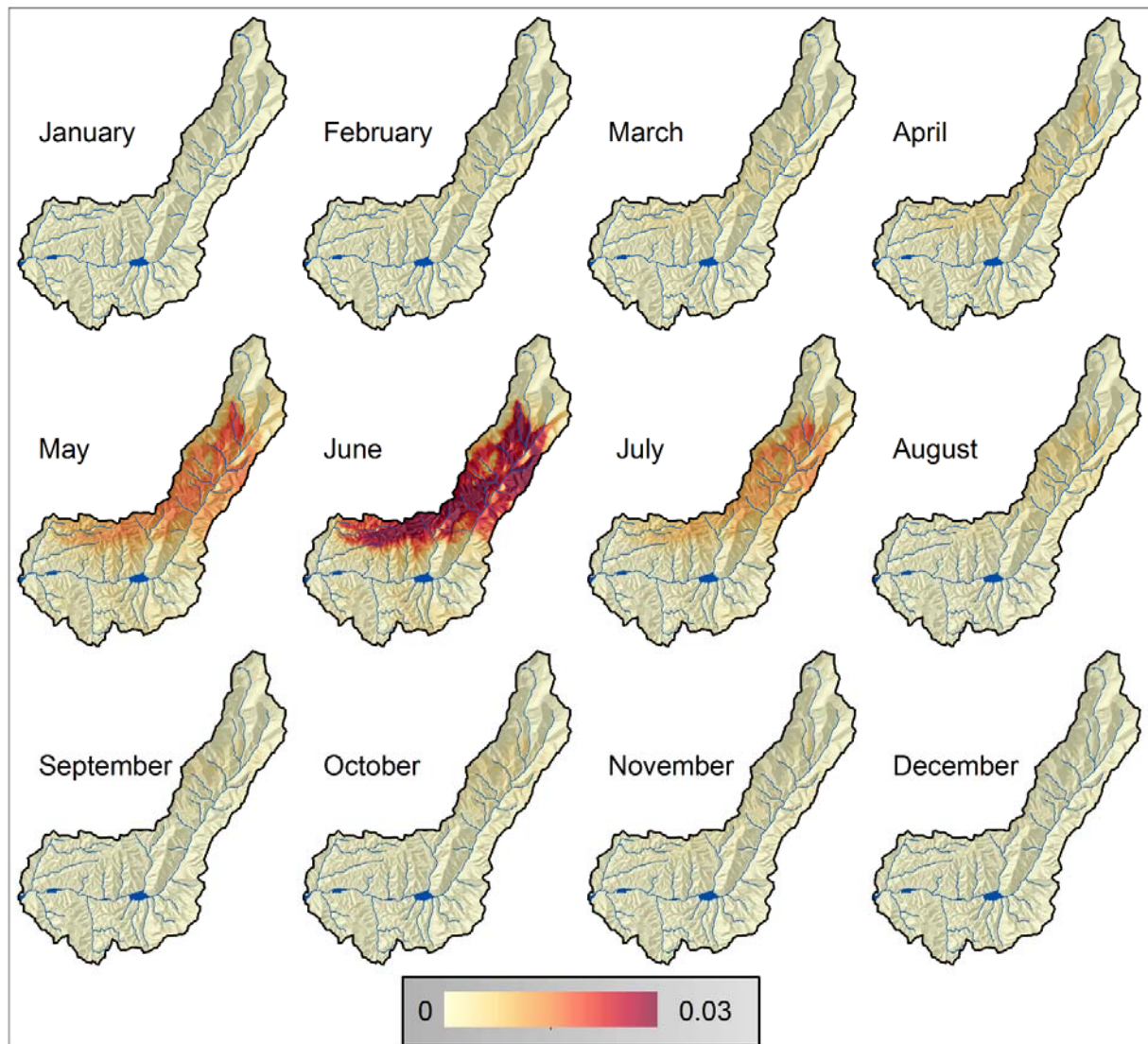


Fig. S8. Seasonality of SF fire occurrence with an ignition source rate of 1.0. Values are the proportion of times each pixel experiences fire. Note the scale.

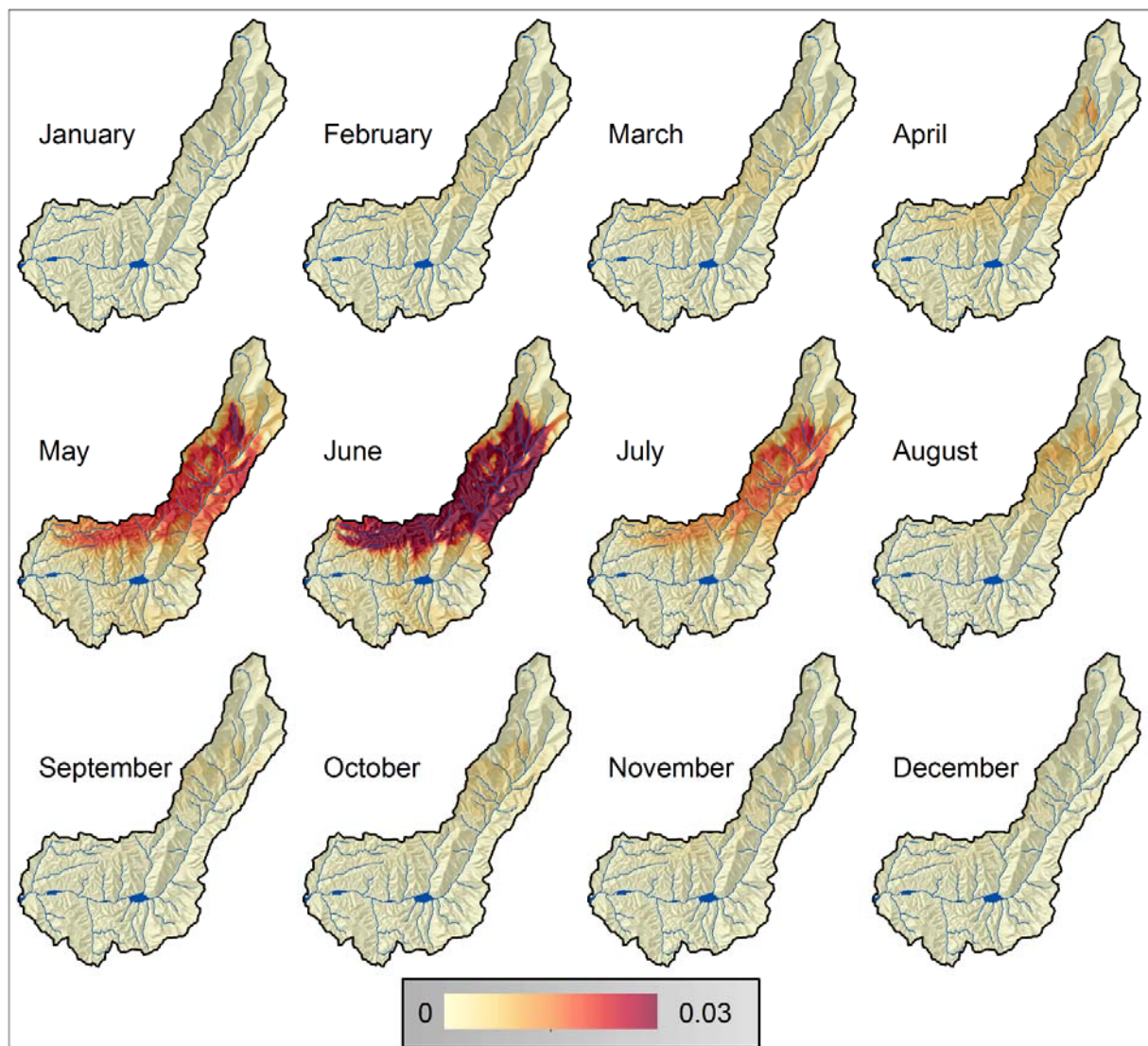


Fig. S9. Seasonality of SF fire occurrence with an ignition source rate of 1.5. Values are the proportion of times each pixel experiences fire. Note the scale.

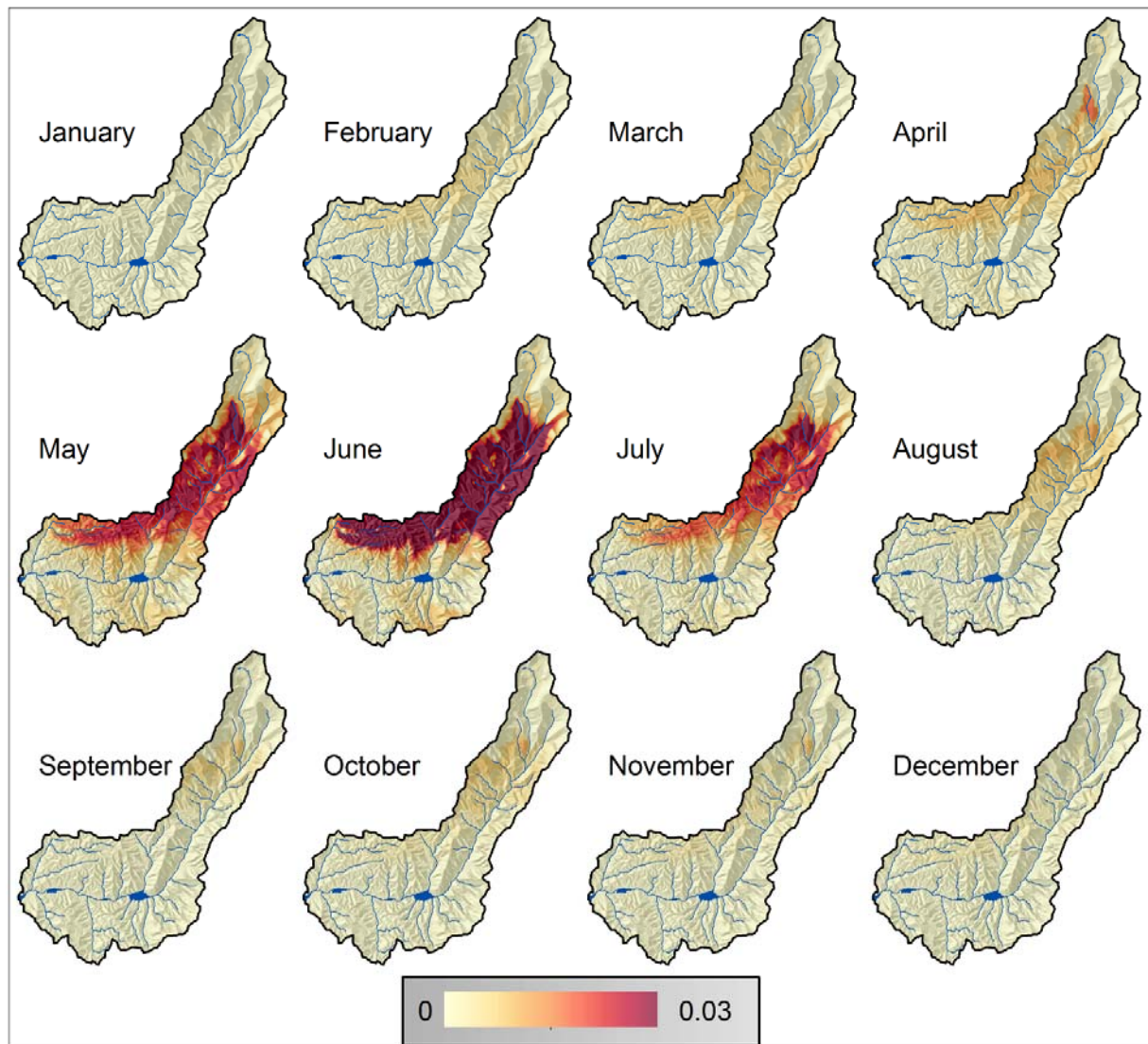


Fig. S10. Seasonality of SF fire occurrence with an ignition source rate of 1.0. Values are the proportion of times each pixel experiences fire. Note the scale.

References

- Garcia ES, Tague CL (2015) Subsurface storage capacity influences climate – evapotranspiration interactions in three western United States catchments. *Hydrology and Earth System Sciences* **19**, 4845–4858 [doi:10.5194/hess-19-4845-2015](https://doi.org/10.5194/hess-19-4845-2015).
- Garcia ES, Tague CL, Choate JS (2013) Influence of spatial temperature estimation method in ecohydrologic modeling in the Western Oregon Cascades. *Water Resources Research* **49**, 1611–1624 [doi:10.1002/wrcr.20140](https://doi.org/10.1002/wrcr.20140).
- LANDFIRE (2014) Fire regime group layer, LANDFIRE 1.4.0. (US Department of the Interior, Geological Survey) Available at <http://LANDFIRE.cr.usgs.gov/viewer/> [Verified 2 March 2017]

- Masseran N, Razali AM, Ibrahim K, Latif MT (2013) Fitting a mixture of von Mises distributions in order to model data on wind direction in peninsular Malaysia. *Energy Conversion and Management* **72**, 94–102 [doi:10.1016/j.enconman.2012.11.025](https://doi.org/10.1016/j.enconman.2012.11.025).
- Tague C, Peng H (2013) The sensitivity of forest water use to the timing of precipitation and snowmelt recharge in the California Sierra: implications for a warming climate. *Journal of Geophysical Research* **118**, 875–887 [10.1002/jgrg.20073](https://doi.org/10.1002/jgrg.20073).
- Tague CL, Choate JS, Grant G (2013) Parameterizing subsurface drainage with geology to improve modeling streamflow responses to climate in data limited environments. *Hydrology and Earth System Sciences* **17**, 341–354 [doi:10.5194/hess-17-341-2013](https://doi.org/10.5194/hess-17-341-2013).